Journal of Alloys and Compounds 509 (2011) 3219–3222

Contents lists available at ScienceDirect

Journal of Alloys and Compounds

journal homepage: www.elsevier.com/locate/jallcom

Magnetic and anomalous transport properties in Fe_2MnAl

Zhuhong Liu[a,*], Xingqiao Ma[a], Fanbin Meng[b], Guangheng Wu[c]

[a] Department of Physics, University of Science and Technology Beijing, Beijing 100083, China
[b] School of Materials Science and Engineering, Hebei University of Technology, Tianjin 300130, China
[c] Beijing National Laboratory for Condensed Matter Physics, Institute of Physics, Chinese Academy of Sciences, Beijing 100080, China

ARTICLE INFO

Article history:
Received 13 October 2010
Received in revised form 8 December 2010
Accepted 9 December 2010
Available online 16 December 2010

Keywords:
Transport properties
Melt-spinning
Heusler alloys
Magnetic properties
Magnetoresistance

ABSTRACT

This study investigated the magnetism and anomalous transport properties of the melt-spun ribbon Fe_2MnAl alloy. It is found that the alloy exhibits ferromagnetic order with the Curie temperature of ~150 K, followed by another magnetic transition at $T_R \sim 51$ K. It is suggested there is antiferromagnetism pinning effect on the ferromagnetic matrix at the temperature below T_R. A steep rise of the resistance below T_R has been observed, which can be understood in terms of antiferromagnetic scattering. An appearance of the resistance maximum near the Curie temperature and the negative temperature dependence of the resistance above Curie temperature are associated with the magnetic phase transition from ferromagnetism to paramagnetism. A negative magnetoresistance at low temperature arising from inhomogeneous magnetic scattering is reported.

1. Introduction

Ternary alloy system Fe–Mn–Al has been extensively investigated for a long time. A lot of work has been focused on the low Mn content in relation to the spin glass state in dilute metallic alloys, such as $Fe_{0.70-x}Mn_xAl_{0.30}$ ($0 \le x \le 0.6$) as a consequence of the presence of competing interactions between ferromagnetic of Fe–Fe coupling and antiferromagnetic of the Fe–Mn, Mn–Mn couplings [1]. Study of $Fe_{89-x}Mn_{11}Al_x$ alloys varying x between 2 and 40 at.% revealed that with increasing the Al concentration, the alloys change their structure from A2, crossing a DO_3 region up to B2 structure [2]. The structural order in this system has great influence on their magnetic properties of the alloys. Corresponding to the above structure, the magnetic properties of the alloys changing from ferromagnetism via a region of re-entrance towards antiferromagnetism have been observed [2]. The magnetic properties in Heusler alloys $Fe_{2+x}Mn_{1-x}Al$ have been investigated [3], showing that the Curie temperature and saturation magnetization increased with the Fe content.

Since the discovery of giant magnetoresistance (GMR) by the groups of Fert [4] and Grunberg et al. [5], a new field in condensed matter, magnetoelectronics or spintronics, has evolved and grown steadily in the last 20 years. As the elements of multilayered magnetoelectronic devices such as the magnetic tunnel junction [6] and the giant magnetoresistance spin valve [7], high-spin polarization materials, especially half-metals, have been attracted much attention. Stoichiometric Heusler alloys Fe_2MnAl has been predicated to be half-metal by band structure calculation [8]. Furthermore, it has been found that melt-spinning is effective in improving the GMR effect due to the induction of the inhomogeneous magnetic entity, i.e. in Cu_2MnAl ribbons [9]. So we choose Fe_2MnAl melt-spun ribbons as the research target. In this paper, we focused on the magnetic and anomalous transport properties. Based on the magnetization measurement, it is suggested there is antiferromagnetic coupling in the ferromagnetic matrix in our sample. A steep rise of resistance at temperature below 51 K arising from antiferromagnetic scattering and a maximum of resistance at Curie temperature has been observed in Fe_2MnAl alloy.

2. Material and method

We prepared the precursor ingot by melting pure metals in proportion in an induction furnace under the argon atmosphere. Subsequently the ingot was melted in a quartz tube and rapidly cooled by spinning onto a copper wheel, spinning at a linear velocity of about 20 m/s. The ribbon is about 30 μm thick. The structure of the ribbons was characterized by means of X-ray diffraction (XRD) using a Philips X'Pert MPD instrument with Cu Kα radiation. The temperature dependence of electrical resistance and magnetoresistance were carried out by standard four-probe technique over the temperature range from 4.2 K to 300 K. A commercial superconducting quantum interference device (SQUID) magnetometer (Quantum Design MPMS) was used to measure the magnetic properties.

3. Results and discussion

3.1. Structure

The chemical structure of the Fe_2MnAl is readily determined using XRD techniques. The intensities of different lattice reflec-

* Corresponding author.
E-mail address: zhliu_info@yahoo.com (Z. Liu).

0925-8388/$ – see front matter © 2011 Elsevier B.V. All rights reserved.
doi:10.1016/j.jallcom.2010.12.070

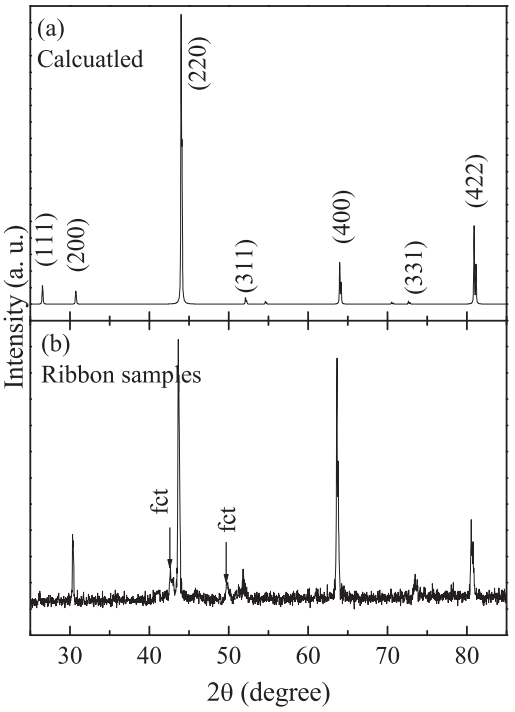

Fig. 1. (a) Calculated X-ray powder diffraction pattern for Heusler alloy Fe_2MnAl; (b) Experimental pattern for Fe_2MnAl melt-spun ribbons.

tions are proportional to the square of the structure factor, F^2. For Heusler alloys X_2YZ, F(1 1 1) reflects the chemical ordering of Y and Z atoms, and F(2 0 0) corresponds to the superlattice reflections of X atoms, while F(2 2 0) is order-independent principal reflections [10]. Fig. 1(a) shows the calculated XRD pattern of Fe_2MnAl powder samples with the experimental lattice constant of $a = 5.816$ Å [11] for ordered $L2_1$ Heusler structure. As expected, the superlattice diffraction peaks of (1 1 1) and (2 0 0) are both presented. The experimental XRD pattern for Fe_2MnAl ribbons is shown in Fig. 1(b). The lack of the (1 1 1) peak indicates a large amount of disordered occupation between Mn and Al. The (2 0 0) superlattice peak indicates the ordering of the Fe sublattice appears. Both characteristics suggest the ribbon sample presents mainly B2 structure. Except the main B2 phase diffraction peaks, extra rather small diffused peaks emerged, as denoted by arrows. According to the previous studies on Fe–Mn–Al ingot samples [3], the two peaks can be identified as minority face centered tetragonal (fct) phase.

3.2. Magnetic properties

Fig. 2 shows the temperature dependence of the magnetization of Fe_2MnAl ribbons measured after zero-field-cooling (ZFC) and field-cooling (FC). Here, the curve marked by ZFC was obtained by cooling the sample from above Curie temperature to 5 K in zero applied field, and then measuring the thermomagnetic curve with increasing temperature in 50 Oe applied field. The curve marked by FC was obtained by cooling the sample from above Curie temperature to 5 K with applied field of 50 Oe, and then increasing temperature in the same applied field as indicated in Fig. 2. For the ZFC curve, a peak at ~51 K denoted as T_R is clearly observed. However the FC-curve at temperature below T_R shows a different behavior. It can be seen that the thermomagnetic curves measured after ZFC and FC exhibit irreversible behavior below T_R. It seems like a spin-glass transition behavior or a magnetic transition. Further increasing temperature, a ferromagnetic to paramagnetic transition is also observed with the transition temperature is ~150 K.

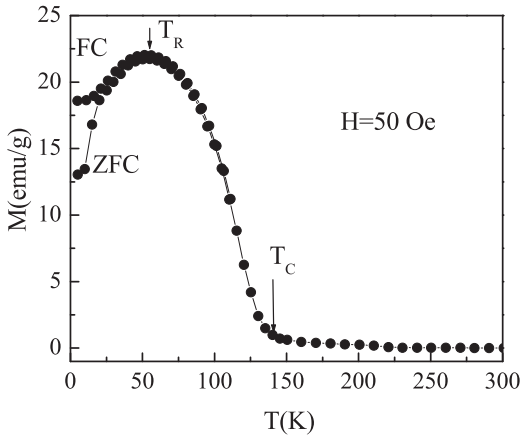

Fig. 2. Temperature dependence of the magnetization of Fe_2MnAl ribbons in 50 Oe under zero-field-cooling and field-cooling conditions.

The arrott plots of the magnetization, namely a plot of the square of the magnetization M as a function of H/M, for Fe_2MnAl melt-spun ribbons are shown in Fig. 3. The data taken at high fields are fitted by straight lines. Extrapolating the linear fit line to zero field, it is found that the intercept is zero at about 150 K, indicating the Curie temperature for Fe_2MnAl is about 150 K, which is consistent with M–T curve. The positive intercept at temperature below 150 K confirmed the existence of the spontaneous magnetization, implying the long range ferromagnetic order indeed exists in the alloys. So the spin-glass transition behavior in our sample can be excluded from these results. We consider the transition at T_R a second magnetic transition. It has been suggested that in magnetically heterogeneous systems, the ZFC and FC splitting for M–T curves that occurs just below a magnetic transition temperature is usually due to the antiferromagnetic pinning effect in the ferromagnetic parts [12,13]. Therefore, an antiferromagnetic entity may exist in this Fe_2MnAl melt spun ribbons.

Fig. 4 shows the magnetic hysteresis loop measured at 5 K for Fe_2MnAl sample. It shows a remanence of 28 emu/g and a coercive force of 370 Oe, indicating an antiferromagnetic ordering might be taking place in the sample as pointed out in Fig. 1. Inset Fig. 4 shows the field dependence of the magnetization $M(H)$ at 5 K. The magnetization does not saturate up to 5 T, suggesting a disordered magnetic system. Together with the observed remanence, it is evident that our sample is inhomogeneous ferromagnetic systems, rather than usual uniform ferromagnets. Buschow et al. show the saturation moment at 4.2 K for Fe_2MnAl ingot treated at 1173 K for 12 days is 1.58 μ_B per formula unit [11]. The magnetization

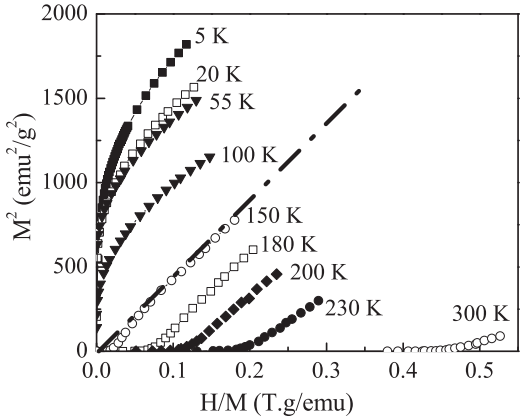

Fig. 3. Arrot plot of M^2 vs. H/M at various temperatures for Fe_2MnAl ribbons.

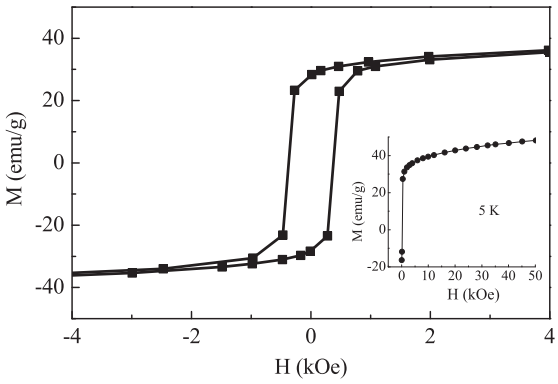

Fig. 4. Magnetization hysteresis curve in the low field range measured at 5 K. Inset graph shows the initial magnetization curve at 5 K.

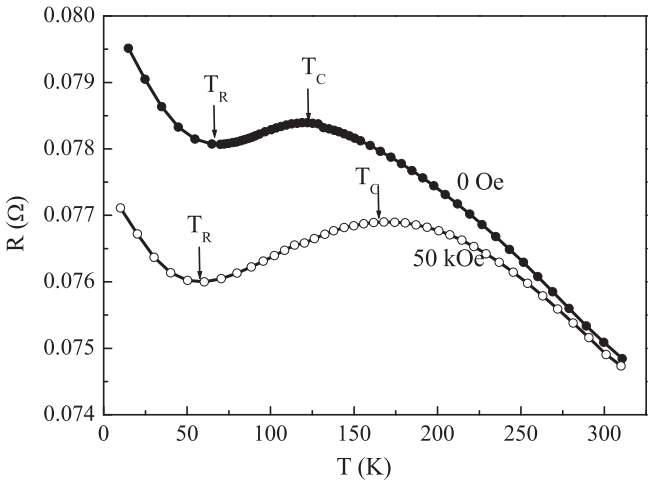

Fig. 5. Temperature dependence of resistance at different fields.

moment of our Fe_2MnAl ribbon at 5 K is 38 emu/g (equivalent to 1.32 μ_B per formula unit) obtained by extrapolating high field *M–H* curve to zero field, which is smaller than that reported in literature 11, manifesting the decrease of magnetic ordering caused by melt-spinning.

Paduani et al. have reported the magnetic properties of Fe_2MnAl arc-melting ingot sample [3]. Comparing with our experiment results, although ZFC and FC splitting has also been observed in their sample, there is no peak temperature in their sample. The Curie temperature for the ingot sample is 300 K, much higher than our ribbon sample. Furthermore, there is no magnetic hysteresis and remanence for their sample. This is probably due to different sample preparation method. For Heusler alloy Fe_2MnAl, the Mn and Al atoms prefer to sit on the 4b sites (Wyckoff notation) of the cubic cell of the Fm3m structure. However, a random distribution can easily occur, especially when the sample was prepared with a non-equilibrium solidifying method, such as melt-spinning in our case [10]. As confirmed by the XRD results shown in Fig. 1, the Mn–Al disorder occurs to a large extent in our ribbon samples. It is known that the Mn–Mn interaction is strongly dependent on their distance in Heusler alloy [14]. The Mn atoms are antiferromagnetically coupled to the Mn atoms in Al site and ferromagnetically coupled to Mn in their own occupation. Magnetic clusters arising from the antisite may form in the sample. A competition of ferromagnetic interactions and antiferromagnetic interactions resulted in a magnetically inhomogeneous state. The higher Curie temperature of the arc-melting sample reported in the Ref. [3] provided further evidence for the improvement of ferromagnetic Mn–Mn interaction of the ingot sample.

3.3. Transport properties

Fig. 5 shows the temperature dependence of resistance in the temperature range of 5–300 K measured under the field of 0 and 50 kOe, respectively. Without the external field, the resistance slope d*R*/d*T* is negative below the transition temperature T_R and a semiconducting behavior was observed. Oppositely, between T_R and T_C, d*R*/d*T* is positive, which means the metallic behavior of the sample. Above T_C, d*R*/d*T* turns to negative again. It is obvious that *R–T* curves exhibit anomalies at both T_R and T_C. The anomaly at T_R demonstrates there is a magnetic transition at this temperature. As discussed above, the sample below T_R presents ferromagnetic average, but antiferromagnetic phase is coexistence with the ferromagnetic matrix. It is reasonable to suppose the crossover between the metallic and semiconducting behaviors at T_R is associated with antiferromagnetism scattering arising from the effective number of conduction electron density decreases due to a truncation of the Fermi surface [15].

The metallic property transformed to semiconducting property accompanying with the magnetic transition from ferromagnetic to paramagnetic. This suggested that the resistance maximum at 125 K is triggered by magnetic ordering transition. It is known that the resistivity can be expressed as below [16]:

$$\rho = \rho_0 + \rho_{ph}(T) + \rho_m(T),$$

where ρ_0 is residual resistivity, $\rho_{ph}(T)$ represents the contribution of phonon scattering to the resistivity, $\rho_m(T)$ is the magnetic scattering term. Generally speaking, $\rho_{ph}(T)$ increases with increasing temperature. The magnetic scattering is proportional to $M(0)^2$–$M(T)^2$, $M(0)$ and $M(T)$ are the saturation magnetization at 0 K and *T* K, respectively. In this regular way, the disappearance of the temperature dependence of electron–magnon scattering above T_C resulted in the magnetic scattering reaches its maximum as the temperature increased to T_C. Therefore, the resistance should increase above T_C. However, it is contradict with our experiment fact that there is an anomalous decrease of resistance above T_C, as has been observed in $Fe_{3-x}V_xGa$, $Fe_{3-x}Ti_xGa$, $Fe_{3-x}M_xSi$(M = triansition 3d metal) and $Fe_{3-x}V_xAl$ [16–18]. It is proposed this phenomenon is related to the strong magnetic scattering in these systems [16].

Under the effect of 50 kOe, the resistance is suppressed significantly below Curie temperature and T_C shifts to higher temperature. This suggests that the short-range magnetic disordering inside the inhomogeneous magnetic materials is ferromagnetic aligned in some extent under the external magnetic field which enhances the Curie temperature and decreases the resistance largely.

Fig. 6 shows the magnitude of the longitudinal magnetoresistance (*MR*) as a function of the applied magnetic field. The *MR* is defined as

$$MR = \frac{\Delta R}{R} = \frac{R(H) - R(0)}{R(0)},$$

where $R(H)$ is the resistance of the sample in a magnetic field *H* and $R(0)$ is the resistance without field. The *MR* value is negative in all measured temperature. The magnitude of *MR* increases upon increasing the field and no sign of saturation. The *MR* value at 50 kOe increased with decreasing field and reaches its maximum of about 3% at 30 K. According to the XRD results, the main phase for our ribbon sample is B2 phase, in which antiferromagnetic and ferromagnetic interaction between Mn–Mn atoms are coexistence. Simultaneously, there are minor fct precipitates in the mainly B2 phase. These suggest our sample is magnetic inhomogeneous mate-

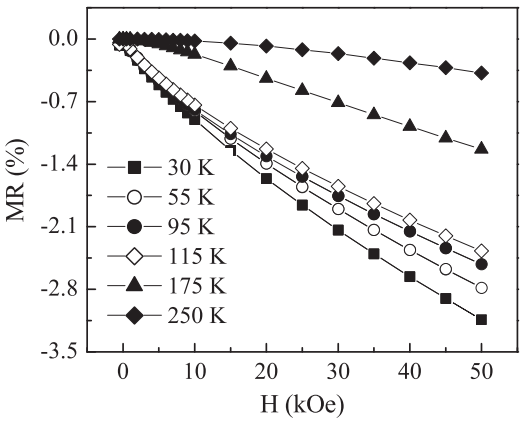

Fig. 6. The magnetic field dependence of *MR* at various temperatures.

rials. Magnetic measurement implies antiferromagnetic coupling exists in the ferromagnetic matrix. These antiferromagnetic have random magnetization directions in zero field, giving rise to strong spin-dependent scattering. An external magnetic field will align the magnetization direction. Consequently, spin-dependent scattering is suppressed, resulting in negative *MR*. It should be pointed out that antiferromagnetic coupling spins between Mn atoms are still antiparallel, but point to the field direction.

4. Conclusions

To sum up, in this paper we have systemically investigated the magnetic and anomalous transport behavior in Fe_2MnAl melt-spun ribbons. The experiments showed definitely the connection between the electrical resistance anomaly and the magnetic structure. A semiconductor–metal transition and a metal–semiconductor transition are corresponding to T_R and T_C, respectively. The negative slope of resistance below T_R is attributed to the antiferromagnetic scattering. There is a maximum of resistance at T_C, which is arising from the strong magnetic scattering. A negative *MR* due to the spin-dependent scattering is observed in the ribbon samples.

Acknowledgement

The authors wish to acknowledge the financial supports by National Natural Science Foundation of China in Grant Nos. 10774178 and 50971055.

References

[1] K.A. Azez, M.K. Hasan Qaseer, I.A. Al-Omari, J. Alloys Compd. 85 (2003) 4358.
[2] H. Bremers, J. Hesse, H. Ahlers, J. Sievert, D. Zachmann, J. Alloys Compd. 366 (2004) 67.
[3] C. Paduani, A. Migliavacca, W.E. Pöttker, J. Schaf, J.C. Krause, J.D. Ardisson, C.A. Samudio Pérez, A.Y. Takeuchi, M.I. Yoshida, Phys. B 398 (2007) 60.
[4] M.N. Baibich, J.M. Broto, A. Fert, F. Nguyen Van Dau, F. Petroff, P. Eitenne, G. Creuzet, A. Friederich, J. Chazelas, Phys. Rev. Lett. 61 (1988) 2472.
[5] G. Binasch, P. Grunberg, F. Saurenbach, W. Zinn, Phys. Rev. B 39 (1989) 4828.
[6] J.S. Moodera, L.R. Kinder, T.M. Wong, R. Meservey, Phys. Rev. Lett. 74 (1995) 3273.
[7] B. Dieny, V.S. Speriosu, S.S.P. Parkin, B.A. Gurney, D.R. Wilhoit, D. Mauri, Phys. Rev. B 43 (1991) 1297.
[8] S. Fjuii, S. Ishida, S. Asano, J. Phys. Soc. Jpn. 64 (1995) 185.
[9] L. Yiping, A. Murthy, G.C. Hadjipanayis, H. Wan, Phys. Rev. B 54 (1996) 3033.
[10] P.J. Webster, Contemp. Phys. 10 (1969) 559.
[11] K.H.J. Buschow, P.G. van Engen, J. Magn. Magn. Mater. 25 (1981) 90.
[12] M. Acet, E. Duman, E.F. Wassermann, L. Manõsa, A. Planes, J. Appl. Phys. 92 (2002) 3867.
[13] E. Duman, M. Acet, Y. Elerman, A. Elmali, E.F. Wassermann, J. Magn. Magn. Mater. 238 (2002) 11.
[14] J. Enkovaara, O. Heczko, A. Ayuela, R.M. Nieminen, Phys. Rev. B 67 (2003) 212405.
[15] I. Das, E.V. Sampthkumaran, R. Vijayaraghavan, Phys. Rev. B 44 (1999) 159.
[16] N. Kawamiya, Y. Nishino, M. Matsuo, S. Asano, Phys. Rev. B 44 (1991) 12406.
[17] Y. Nishino, H. Sumi, U. Mizutani, Phys. Rev. B 71 (2005) 094425.
[18] A. Matsushita, T. Naka, Y. Takano, T. Takeuchi, T. Shishido, Phys. Rev. B 65 (2002) 075204.